APS physics

CHORUS

This is the accepted manuscript made available via CHORUS. The article has been published as:

Nonlocal entanglement and directional correlations of primordial perturbations on the inflationary horizon

Craig Hogan

Phys. Rev. D **99**, 063531 — Published 25 March 2019

DOI: 10.1103/PhysRevD.99.063531

FERMILAB-PUB-18-178-A

Nonlocal Entanglement and Directional Correlations of Primordial Perturbations on the Inflationary Horizon

Craig Hogan
University of Chicago and Fermilab

Models are developed to estimate properties of relic cosmic perturbations with "spooky" nonlocal correlations on the inflationary horizon, analogous to those previously posited for information on black hole event horizons. Scalar curvature perturbations are estimated to emerge with a dimensionless power spectral density $\Delta_S^2 \approx Ht_P$, the product of inflationary expansion rate H with Planck time t_P, larger than standard inflaton fluctuations. Current measurements of the spectrum are used to derive constraints on parameters of the effective potential in a slow-roll background. It is shown that spooky nonlocality generically creates statistically homogeneous and isotropic primordial curvature perturbations that are initially exactly directionally antisymmetric. New statistical estimators are developed to study unique signatures in CMB anisotropy and large scale galaxy surveys.

I. INTRODUCTION

Cosmic perturbations on the largest scales are widely thought to come from microscopic quantum fluctuations on the horizon scale during inflation. This hypothesis is supported by a unique and precisely measured experimental signature, a power spectrum of primordial curvature perturbations on very large scales that is almost but not exactly scale-free[1–6].

To account for these data, slow-roll inflation[7–9] posits a classical background universe that expands nearly exponentially according to classical general relativity, driven by the free energy density $V(\phi)$ of a nearly-uniform scalar field with a slowly time-varying classical expectation value, ϕ. In this setting, the quantum model that leads to perturbations is adapted from high energy particle physics: curvature perturbations are produced by the gravitation of quantum field fluctuations when they freeze out on the inflationary horizon scale. Standard inflation models assume that quantum geometrical degrees of freedom behave like those of quantum fields, and that classical properties of space and time are well defined and determinate on all scales.

A new hypothesis about the primordial quantum system is explored here: *the background geometry is assumed to be classical only after each scale leaves the horizon.* Before then, even properties of space and time that are universal to all classical metrics, such as a local inertial frame, are allowed to be nonlocal and indeterminate, so perturbations can emerge with new kinds of "spooky" nonlocal correlations that are classically impossible. The standard model of inflation and linear perturbation mode evolution is still assumed on all scales after they exit the inflationary horizon.

In this scenario, *the inflationary horizon is a quantum object: a causal null surface whose correlations are nonlocal in space and time.* In standard inflation, quantized states of the field vacuum evolve in a classical space-time background. Here, the early sub-horizon-scale geometry is allowed to be indeterminate, with spooky nonlocal correlations of geometrical degrees of freedom everywhere on the horizon. Similar nonlocal quantum coherence of horizon states has been invoked to resolve information paradoxes in evaporating particle states that create back reaction on black hole event horizons[10–12].

In this model, the origin of cosmic perturbations is not separate from the emergence of locality and of space-time itself from a quantum system. Classical space-time, along with its local inertial frame and the local cosmic standard of rest, emerge together as a holistic process. On the inflationary horizon, geometrical quantum states are nonlocal and include new kinds of entanglement among all directions. The emergent perturbations of classical invariant curvature display previously-neglected, nonlocally correlated noise. Their nonlocal, multidirectional correlations on the horizon can have measurable physical effects on the amplitudes and phases of relic perturbations.

Specific properties of spooky correlations are estimated here by adapting covariant models of locality, emergence, and entanglement previously developed to design and interpret laboratory experiments[13–15], based on Planck scale quantum states with nonlocal correlations that extend everywhere on light cones or spacelike causal diamond surfaces. The relic curvature perturbations are estimated to exceed the standard, inflaton-generated perturbations by a significant factor. The estimated emergent perturbation spectrum agrees with current measurements. The model has fewer parameters than standard inflation models, since perturbations arise from a quantum-geometrical effect that is not sensitive to properties of the matter fields.

Some still-untested predictions differ nontrivially from standard inflation. Signatures of spooky primordial correlations can survive in cosmic density perturbations today, in particular, a new kind of scale-free directional antisymmetry that violates locality at inflation. Specific model-independent statistical tests can distinguish spooky correlations from standard perturbations on scales still in the linear regime. It is suggested below

that they might already be detected in CMB anistropy, and if so, that it may be possible to detect them with new kinds of measurements with large scale galaxy surveys.

II. SPOOKY INFLATION

A. Homogeneous classical inflation

A standard inflation model[7–9] is assumed throughout this paper for the classical background cosmology. The model of mass-energy is a spatially uniform classical (that is, unquantized) inflaton field, with dimension of mass and vacuum expectation value $\phi(t)$, where t is a standard FRW time coordinate. In standard notation where $\hbar = c = 1$, the expansion rate H and cosmic scale factor a evolve according to classical general relativity and thermodynamics,

$$H^2(t) \equiv (\dot{a}/a)^2 = (8\pi G/3)(V(\phi) + \dot{\phi}^2/2), \qquad (1)$$

where the evolution of the inflaton depends on the potential $V(\phi)$ via

$$\ddot{\phi} + 3H\dot{\phi} + V' = 0, \qquad (2)$$

and $V' \equiv dV/d\phi$. During slow roll inflation, the evolution of ϕ approximately obeys

$$3H\dot{\phi} \approx -V', \qquad (3)$$

which produces a nearly-exponential expansion. About 60 e-foldings in a after the currently observable volume of the universe matches the scale c/H of the inflationary horizon, inflation ends, and subsequently "reheats" with the conversion of ϕ to other forms of matter.

Quantum fluctuations of the inflaton, although they are presumably still present for a physical inflaton field, are neglected here; as shown below, their gravitational effect is smaller than the spooky geometrical perturbations. As usual, perturbations of wavenumber k freeze in at the cosmic scale factor $a(k)$ when $k = a(k)H(k)/c$.

The background evolution at late times is assumed to be the standard concordance ΛCDM model. This standard background solution provides the global definition of surfaces of unperturbed cosmic time on comoving world lines, corresponding to surfaces where ϕ is constant.

B. Spooky correlations in emergent gravity

At the most basic level, quantum mechanics is a theory of correlations that does not assume any particular projection onto space and time. It is possible, as envisioned in relational (or "emergent") quantum gravity, that locality— the relationship that differentiates space-time positions or events— emerges as an approximate observable in a quantum system[16–18]. In general, relational quantum gravitational degrees of freedom and correlations differ from those of fields. They can produce quantum fluctuations associated with nonlocal correlations of positional relationships on all scales.

1. Precedents for nonlocal correlations of quantum geometry

Theoretical studies, especially of systems with horizons, have long hinted that space-time relationships are encoded in entanglement information, analogous to spooky macroscopic correlations of entangled particle states. If space and time emerge from a quantum system, a new kind of nonlocal correlation on all scales is needed to account for finite and holographic gravitational information in black holes[19–21]; its generalization to a "holographic principle" in any space-time[22–24]; consistent evolution of matter fields and information flow in the presence of black hole horizons[10–12] without information paradoxes[25]; the absence of field states more massive than black holes in a volume of any size[26]; and holographic correlations in anti-de Sitter space[27–30].

These results suggest that information in quantum geometrical degrees of freedom is less localized, and more universally entangled, than that in particles and fields, even though it is governed by a much smaller dimensional scale, the Planck time $t_P \equiv \sqrt{\hbar G/c^5} = 5.4 \times 10^{-44}$sec. It is even possible to derive general relativity thermodynamically, as a statistical theory or equation of state[31–34], where the basic elements are invariant null surfaces, such as horizons, light cones, and causal diamonds[22–24]. As elegantly prefigured by Wheeler[35], "...in the gravitational theory we should be able in principle to dispense with the concepts of space and time and take as the basis of our description of nature the elementary concepts of world line and light cone."

2. Physical effects of exotic correlations

The previous considerations are all of a general, abstract nature. No consensus exists about concrete physical effects of exotic holographic geometrical correlations on large scales, and no experimental departure from classical space-time has been convincingly demonstrated. Even so, there are theoretical and experimental constraints on the specific form exotic correlations can take.

In standard quantum mechanics, "spooky action at a distance" refers to nonlocal quantum correlations of entangled particle states that extend indefinitely in the future of an event where a state is prepared[36, 37]. For example, in positron emission tomography, the space-time position of an annihilation event can be reconstructed, in principle with diffraction-limited fidelity, from a macroscopic correlation in arrival times and positions of a pair

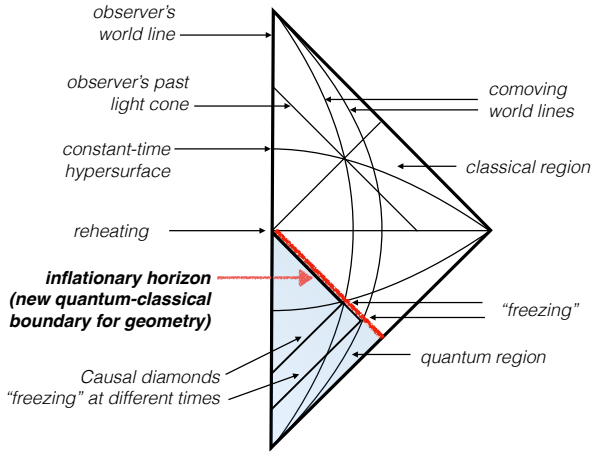

FIG. 1. Penrose diagram of the standard inflationary ΛCDM universe. Constant time and space surfaces are shown in comoving coordinates. In the spooky scenario, the quantum-classical boundary for geometry lies on an observer's inflationary horizon, the null surface represented by the upper boundary of the shaded region. Entanglement on the horizon creates new, delocalized spooky correlations of perturbations among different scales and spatial directions.

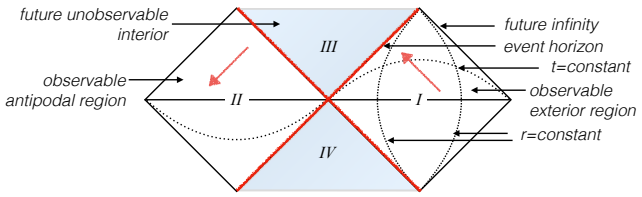

FIG. 2. Maximally extended Penrose diagram of an eternal Schwarzschild black hole, adapted from ref. [10]. Surfaces of constant time t and radius r are shown for Schwarzschild coordinates that approach proper coordinates for a distant external observer. Entanglement on the horizon creates globally delocalized correlations between positions and momenta of incoming and outgoing particle states, time-antisymmetric between antipodal regions I and II, as indicated by bold arrows. In spooky inflation, similar antipodal time antisymmetry on the inflationary horizon leads to directionally antisymmetric scalar curvature perturbations.

of entangled photons traveling in opposite directions anywhere on its future light cone.

Entangled particle pairs act as sources for superpositions of gravitational states, so geometry itself must also have spooky nonlocal correlations on light cones. Unlike the particle example, geometrical states are universal: they must entangle with all forms of matter and energy on a light cone in all directions, not just a single pair of particles. Their correlations describe the relationship of the local inertial frame of a world line to the rest of the universe[13–15].

Exotic correlations of geometry must exist in flat space-time as well as black holes, so they should affect states of light in the laboratory. They could have escaped experimental detection because the estimated correlation scale is very small— comparable not to the Planck length, but to the diffraction width of a Planck bandwidth wave function[38]. Even so, they might be measurable with new kinds of experiments[39–42]. Indeed, experimental constraints on symmetries of Planck scale tensor-like holographic correlations[43, 44] are used below to constrain predictions of tensor modes in spooky primordial perturbations.

3. *Quantum models of inflationary fluctuations*

Calculations of perturbations in standard inflation use a model quantum system based on local quantum field theories originally developed for high energy particle interactions (e.g., ref. [45]). The quantized system is the amplitude of a field in space-time, often described as a superposition of modes, each one of which approximates a quantized harmonic oscillator. The standard model system violates locality in a particular way: each mode has built-in spacelike correlations, the classical spatial structure of a plane wave with a certain wavenumber. In standard calculations, this is often expressed mathematically by writing the initial state as a field vacuum state in comoving coordinates.

This model quantum system is not adequate to include all the correlations that could occur among space-time degrees of freedom. The background space-time is classical, meaning that positional relationships are described by commuting quantities. The same classical locality is assigned to quantum fields and their gravitational effects: although the amplitudes are quantized, the comoving field modes have a determinate, globally-defined spatial structure that is shared by the relic metric perturbations.

The new hypothesis here is that during inflation, locality does not apply down to the Planck scale, only down to the horizon scale. Before then, space-time is not constrained to be a classical differentiable manifold. Primordial correlations can violate locality in new ways: relative positions and proper times of comoving world lines emerge with spatially nonlocal correlations on the horizon when they become classical.

The new quantum-classical boundary for perturbations is shown in Fig. (1). It is defined by the classical causal structure around each observer. The "outgoing" states are represented by world lines when they pass through the horizon and their relationships become classical. In the inflationary context, freezing of perturbations is the equivalent of collapse or measurement in the laboratory, and outgoing states (*i.e.*, the positions of world lines) are entangled with each other everywhere on the horizon. In this respect, the nonlocal entanglement of per-

turbations emerging from inflationary horizon states resembles global entanglement of incoming and outgoing particle states emerging from black hole horizons, introduced to solve information paradoxes[10–12]. An eternal black hole horizon (Fig. 2) creates directionally antisymmetric correlations among particle states from quantum back reaction; in spooky inflation, the horizon creates directionally antisymmetric curvature perturbations.

In standard inflation, the quantum-classical boundary is the same for all observers: each plane wave mode of fixed comoving size and direction "freezes" everywhere at the same comoving time, with spatial relationships among world lines determined by a determinate classical background. Here, the emergent space-time hypothesis implies an observer-dependent boundary of the horizon and the quantum region. For any two world lines, their classical positions only freeze in when they pass through each others' horizons, at a time specific to their locations and separation direction. This indeterminacy allows a nonlocal spacelike entanglement among different directions that cannot occur for standard field modes.

The main goal of this paper is to show that it is possible to incorporate these new features into a consistent model for emergent classical perturbations. The models developed here allow sharper predictions than previous generic estimates of holographic discreteness effects on inflation[46, 47]. As shown below, spooky quantum fluctuations project onto observable modes in a way that introduces larger perturbations than usual, and introduces previously-forbidden antisymmetric correlations.

Ultimately, a full theory will require a new quantum model that can include interference in three directions and a model of freezing that can account for the classical causal structure and local inertial frame that emerges for each world-line. A model of quantum-geometrical states cannot be based on a standard correspondence principle, since they represent new unknown quantum degrees of freedom of emergent space and time. Here, simple models are developed based on constraints from matching to classical symmetries— first for causal diamonds in flat space-time, later for a cosmological background. For the present purpose, it does not matter that the degrees of freedom of the models are not "fundamental" in the sense of relational quantum gravity[17]: here, they simply serve to compute correlations among measurements, in the same way as quantum models used to interpret many laboratory systems (*e.g.*, refs. [36, 37]).

C. Quantum-spin-algebra model

The following model is developed to provide a concrete worked example of new quantum-geometrical correlations on scales much larger than the Planck length. The goal is to develop a quantum model for emergent proper time relationships with a world line in flat space-time. More specifically, we need a quantum model with operators that describe the relationships between time on different world lines in different space-time directions. Taking our cue from Wheeler, the quantum states of the model should live on light cones, meaning that causal relationships in all directions define an exact symmetry.

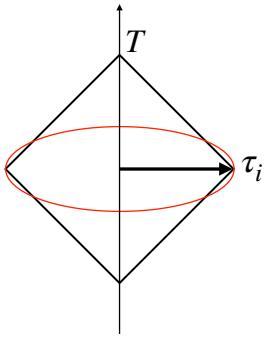

FIG. 3. Space-time diagram of a causal diamond associated with an interval on a world line, shown here in the rest frame. Operators of spin model quantum states correspond to three noncommuting directional components of time, $\hat{\tau}_i$, which combine to form a commuting operator $\hat{T}$, the total duration along the interval in classical proper time. They describe positional relationships between an observer and events on the 2D spacelike boundary in different directions.

Classical proper time is a scalar, but causal relationships defined by a light cone are multidirectional. In the quantum system, these requirements can be reconciled if states in different spatial directions are entangled. All observables in scalar proper classical time should emerge by contracting nonlocal, orientated states in three spatial directions into a scalar clock operator.

These properties motivate us to model quantum space-time relationships using a spin algebra, instead of the quantized harmonic oscillation of scalar amplitude usually used for inflation. The spin model allows a quantitative estimate of new spooky quantum geometrical relationships that cannot occur in standard theory: nonlocal entanglement among multidirectional temporal states, with the correct (Planck-scale, holographic) number of degrees of freedom, for a region of any size.

The standard quantum spin algebra is repurposed here as a relational holographic quantum model of a causal diamond, the region defined by future and past light cones from an interval of time on any world line (Fig. 3). Fluctuations of the quantum system are interpreted as geometrical fluctuations of proper time on a world line relative to the 2D spacelike boundary where the light cones intersect— spooky correlations among directions. The temporal correlations on causal diamonds are extrapolated below to scalar curvature on inflationary horizons, and ultimately to distinctive new exotic properties of the matching relic classical perturbations.

The model is defined by quantum operators $\hat{\tau}_i$ with the dimension of time. The indices i, j, k take the values $1, 2, 3$, identified physically with classical directions in 3-space. The commutation of the operators obey a standard spin algebra in three dimensions:

$$[\hat{\tau}_i, \hat{\tau}_j] = it_P \hat{\tau}_k \epsilon_{ijk}, \tag{4}$$

where ϵ_{ijk} denotes the Levi-Civita antisymmetric 3-tensor. The operators are well known to obey the Jacobi identities

$$[\hat{\tau}_i, [\hat{\tau}_j, \hat{\tau}_k]] + [\hat{\tau}_k, [\hat{\tau}_i, \hat{\tau}_j]] + [\hat{\tau}_j, [\hat{\tau}_k, \hat{\tau}_i]] = 0, \tag{5}$$

so that the quantum theory is self-consistent.

The quantum operator notation $\hat{\tau}_i$ is introduced to highlight our unconventional physical adaptation[48] of this familiar system to describe the quantum entanglement among nonlocal quantum degrees of freedom that emerge as space and time. Instead of angular momentum components, the conjugate variables are directional components of a quantum operator that approximates time in a classical limit, but has noncommuting relationships among spatial directions. With this physical interpretation, Eq. (4) describes a holographic entanglement of geometrical degrees of freedom over an entire 4-volume.

In Eq. (4), the Planck time t_P takes the place of the usual quantum of action, Planck's constant $\hbar$, that governs standard quantum-dynamical relationships associated with displacement operators in a continuous spacetime background. As explained below, the coefficient t_P is chosen so that the number of degrees of freedom agrees with what is needed to produce holographic emergent gravity as a statistical behavior[31–34].

The model posits that quantum spacetime states for a causal diamond much larger than the Planck time ($T >> t_P$) have the same discrete relationships as quantum states for any high angular momentum system ($|J| >> \hbar$). The amplitude, symmetries, and entanglement of fluctuations in emergent time and direction are derived with only quantum commutators: they do not depend on dynamical operators or a Hamiltonian. In standard treatments of angular momentum[49], the quantum conditions (Eq. 4) are often derived from a correspondence principle with classical Poisson brackets; here, they are motivated just from their symmetry and holographic information content.

The spin algebra combines operators associated with three spatial directions into a rotationally invariant algebra. In this interpretation it describes a state in relation to a chosen spatial location, the origin of coordinates, interpreted as a clock or observer at rest. Like an atomic model, the properties of the quantum system are expressed using classical coordinates. The interpretation is extended below to model the emergence of global directions and cosmic time, and the projection of the quantum fluctuations onto classical cosmological perturbations that arise during inflation.

1. *Eigenstates of emergent proper time duration*

Emergent classical proper time duration is described by an operator $\hat{T}$, analogous to total angular momentum:

$$\hat{T}^2 \equiv \hat{\tau}_i^* \hat{\tau}_i \ . \tag{6}$$

In the same way that total angular momentum commutes with all of its components,

$$[\hat{T}^2, \hat{\tau}_i] = 0, \tag{7}$$

the emergent proper time duration T, the observable defined by eigenvalues of $\hat{T}$, has no quantum uncertainty. Causal structure is an exact symmetry by construction: the radius of the 2D boundary (of the causal diamond) in the observer rest frame is identified with cT. Thus, the spin algebra in 3D space actually describes a quantum model of all states in a 4D causal diamond, including the embedded causal diamonds that can nest within it.

Adapting conventional notation for angular momentum, let quantum numbers l denote positive integers that label discrete temporal eigenstates:

$$\hat{T}^2 |l\rangle = l(l+1) t_P^2 |l\rangle, \tag{8}$$

corresponding to discrete eigenvalues of classical proper time duration,

$$T = \sqrt{l(l+1)}\, t_P. \tag{9}$$

2. *Uncertainty relation for orthogonal directions*

The directional operators $\hat{\tau}_i$ are related by an uncertainty relation: a variance $\langle \tau_\perp^2 \rangle = T t_P$ in orthogonal directions that increases with size, in the same way that a state of definite angular momentum in one direction is a superposition of states in the orthogonal directions.

To show this, consider projections of the operator $\hat{\tau}_i$. Let l_i denote its eigenvalues in direction i:

$$\hat{\tau}_i |l, l_i\rangle = l_i t_P |l, l_i\rangle. \tag{10}$$

In a state $|l\rangle$, the operator $\hat{\tau}_i$ can take discrete eigenvalues in units of t_P,

$$l_i = l, l-1, \ldots, -l, \tag{11}$$

giving $2l + 1$ possible values.

Still following standard practice (*i.e.*, ref. [49]), define raising and lowering operators for components in each direction:

$$\hat{\delta}_{1\pm} \equiv \hat{\tau}_2 \pm i\hat{\tau}_3, \tag{12}$$

with equivalent expressions for cyclic permutations of the indices. The effect on a state is to raise or lower the quantum number of the projection onto that component

by one unit (that is, one Planck time), while leaving the total T invariant. In our interpretation, these operators are identified below as discrete, differential, directional projections on individual line cones (e.g., Fig. 5), and in the Appendix, as operators that relate proper time between different world lines.

The duration operator $\hat{T}^2$ can be written in terms of any single i as

$$\hat{T}^2 = \hat{\delta}_{i+}\hat{\delta}_{i-} + \hat{\tau}_i^2 + \hat{\tau}_i = \hat{\delta}_{i-}\hat{\delta}_{i+} - \hat{\tau}_i^2 + \hat{\tau}_i. \quad (13)$$

Direct calculation (e.g., ref.[49]) then leads to the following product of amplitudes for measurements of either of the orthogonal components $\hat{\tau}_j$, with $j \neq i$:

$$\langle l_i|\hat{\tau}_j|l_i-1\rangle\langle l_i-1|\hat{\tau}_j|l_i\rangle = (l+l_i)(l-l_i+1)t_P^2/2, \quad (14)$$

again for any i.

Notice that the left side represents the expectation in an eigenstate $|l_i\rangle$ of an orthogonal-variance operator,

$$|\hat{\tau}_j|l_i-1\rangle\langle l_i-1|\hat{\tau}_j|. \quad (15)$$

Thus, Eq. (14) gives the expected variance $\langle\Delta\tau_\perp^2\rangle$ in orthogonal components $\hat{\tau}_j$ in an eigenstate $|l_i\rangle$ of definite $\hat{\tau}_i$. This leads to a directional uncertainty relation: from Eqs. (9) and (14) in the limit of $l \approx l_i >> 1$, orthogonal temporal displacements have a variance about a mean value T given by

$$\langle\Delta\tau_\perp^2\rangle = \langle(\tau_\perp - T)^2\rangle = Tt_P. \quad (16)$$

This relation refers to time operators in any pair of orthogonal directions, relative to the 2D causal-diamond boundary of radius cT (Fig. 4).

Thus, time on the boundary, defined in relation to an observer at the origin, is in a superposition of directionally antisymmetric states. A causal diamond or horizon surface is never exactly isotropic, but has directionally correlated, antisymmetric fluctuations.

3. *Physical fluctuations in gravitational potential*

To help clarify the physical interpretation of this strange result, define operators for displacement

$$\Delta\hat{\tau}_i \equiv \hat{\tau}_i - \hat{T} \quad (17)$$

and for dimensionless fractional displacement,

$$\hat{\Delta}_i \equiv \Delta\hat{\tau}_i/T. \quad (18)$$

The latter operator represents a difference in potential associated with direction i at separation cT. Fractional time distortions appear as differences in Δ_i along the three spatial directions that are all correlated with each other.

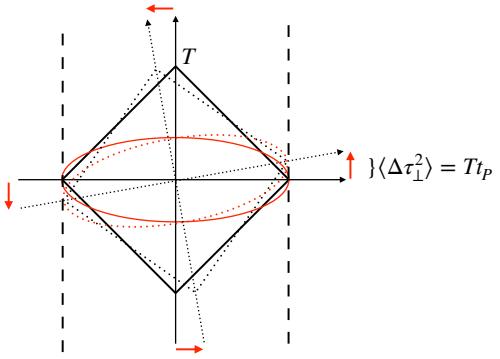

FIG. 4. Visualization of the quantum spin model fluctuations as generalized rotations of a causal diamond. A measurement of time along one axis on the surface of a causal diamond of duration T and radius cT along any direction (here, out of the page) leads to antisymmetric fluctuations of time on the boundary in the orthogonal directions, of magnitude $\langle\Delta\tau_\perp^2\rangle = Tt_P$ (Eq. 16). In the spooky model, antisymmetric fluctuations of curvature (Eq. 19) or proper time (Eq. 58) ultimately freeze in as antisymmetric cosmological perturbations (Eq. 42).

As discussed in the Appendix, the identification of cT with R means that virtual fluctuations in flat space-time are "paid back" on the return light cones, for causal diamonds of any size. Thus, potential fluctuations associated with measurements on a single world line exactly cancel and are not observable. The hypothesis of this paper is that during inflation, nonlocal relational correlations resembling those of $\hat{\Delta}_i$ on different world lines correspond to differences in comoving proper time, or perturbations in scalar curvature in the emergent classical metric on the horizon. This hypothesis has physical consequences.

One physical consequence is a change in the overall amplitude of perturbations. During slow roll inflation, the relevant causal diamond radius is approximately the radius of the horizon, so the fluctuation power of dimensionless relic invariant curvature perturbations is approximately given by

$$\langle\Delta^2\rangle = \langle\Delta\tau_\perp^2\rangle/T^2 = t_P/T = Ht_p. \quad (19)$$

The linear dependence on H is dramatically different from standard non-holographic field-like perturbations, which scale like H^2. The basic reason the geometrical fluctuations are larger than usual is that there are fewer independent degrees of freedom, a direct consequence of holography.

Another physical consequence is a new directional antisymmetry. In the spin-algebra model, it arises because $\hat{\tau}_i$ and $\hat{\Delta}_i$ are odd under parity transformations. The statistical properties of global directional antisymmetry in spooky relic perturbations are derived below from in-

variance on the classical side.

4. Number of eigenstates

The eigenvalues of the time operator $\hat{T}$ are identified with both classical emergent proper time, and with the radius of a causal diamond or horizon of a space-time volume around an observer's world line. This identification reduces the number of independent dimensions by one.

The number of eigenstates within a causal diamond of radius cT can be counted precisely, as if they were discrete angular momentum eigenstates. For each l there are $2l+1$ directional projection eigenstates so the number of degrees of freedom $\mathcal{N}$— interpreted here as the amount of information or entropy in a causal diamond or horizon— scales holographically, as the surface area in Planck units:

$$\mathcal{N} = \sum_{l'=0}^{l} (2l'+1) \approx 2(T/t_P)^2, \tag{20}$$

where the approximation applies in the large l limit, and we have used Eq. (9). The total holographic information of a causal diamond (Eq. 20) counts all the combinations of nested, entangled light cone states that can represent the state of an interval on the world line. Up to factors of order unity in the absolute normalization, this agrees with the entropy of black hole horizons.

5. Semiclassical visualization as light cone fluctuations

In a semiclassical picture where causal diamonds are stitched together from discrete light cones, spooky fluctuations correspond to Planck-scale differential displacements on Planck-proper-time-separated light cones (Fig. 5, and refs. [13–15]). Projections of states are directionally antisymmetric on each light cone, like the rotational raising and lower operators $\hat{\delta}_{i\pm}$, as discussed in the Appendix.

In an inflationary background (Figs. 6 and 7), each light cone imprints a horizon-scale coherent fluctuation when it "freezes" into a classical metric on the horizon. Over an e-folding time, about $(Ht_P)^{-1}$ null surfaces pass through the horizon. Each one has a displacement $\approx t_P$, so the accumulated displacement over a time $1/H$ has a variance $\langle \delta t^2 \rangle \approx t_P/H$. The curvature perturbation is the fractional time dilation associated with the fluctuation on the horizon scale over that time,

$$\Delta_S^2 = \langle \delta t^2 \rangle H^2 = \alpha H t_P, \tag{21}$$

where α is a factor of order unity.

This semiclassical fluctuation picture does not fully capture the weird antisymmetry, nonlocality and entanglement associated with the operators $\hat{\delta}_{i\pm}$ and $\hat{\tau}_i$ in the spin-algebra model of relational emergent time. However, it does lead to the same estimate as Eq. (19) for the amplitude: it depends linearly on the value of H at the time when a fluctuation freezes on the horizon.

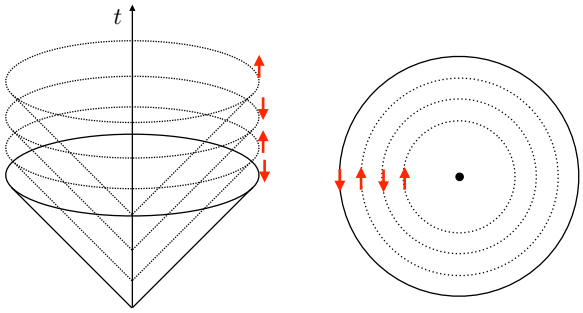

FIG. 5. Foliation of flat space-time, adapted from ref. [15]. Left side: a series of light cones separated by a Planck proper time on an observer's world line. Arrows indicate projections of a raising or lowering operator $\hat{\delta}_{i\pm}$ along some axis (Eq. 12). Right side: light cones at one time in the observer's rest frame.

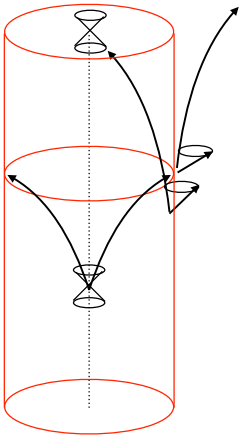

FIG. 6. Radial light trajectories in inflation, shown as proper separation from the world line of an observer (dotted line). During slow roll inflation, the cylinder representing the apparent inflationary horizon, defined by the innermost, outgoing, inbound trajectories, lies at approximately constant proper separation from an observer's world line. It represents the new quantum-classical boundary shown in Fig. (1); outgoing states of perturbations freeze in with nonlocal correlations on this cylinder. Inbound light cones of causal diamonds with a boundary near the horizon entangle with outgoing light cones that freeze significantly later.

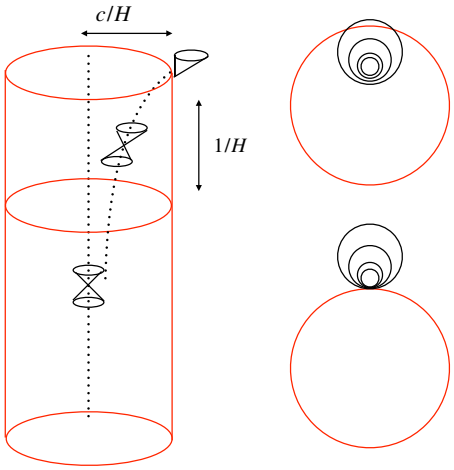

FIG. 7. In the same coordinates as Fig. (6), proper spatial separation of two comoving world lines (dotted) are shown with their light cones. Right side: Multiple time slices are shown of future light cones of two events, one inside and one on the horizon of the observer. In the observer frame, clocks appear to freeze on the horizon.

III. COMPARISON WITH CURRENT MEASUREMENTS

A. Constraints from the perturbation spectrum

Constraints on the parameters of the inflationary background model follow from the result that the curvature perturbation Δ_S^2 on any scale depends only, and linearly, on the value of H when it crosses the horizon (Eqs. 19 and 21). Let ϕ_0 denote the value of ϕ when the measured comoving scales, comparable to the current Hubble length, cross the horizon. From Eqs. (1) and (21),

$$\Delta_S^2 = \alpha(8\pi G t_P^2/3)^{1/2}\ \ V(\phi_0)^{1/2} \tag{22}$$

The measured value[2, 5] $\Delta_S^2 = A_S = 2\times10^{-9}$ implies an energy density during inflation, and an upper limit to reheating temperature, characterized by an energy scale $E_0 = V(\phi_0)^{1/4}$ in Planck units:

$$E_0\ = \alpha^{-1/2}(3/8\pi)^{1/4}\Delta_S\ m_P c^2 \approx 3\times10^{14}\mathrm{GeV}, \tag{23}$$

where $m_P \equiv \sqrt{\hbar c/G}$. As usual the actual reheating temperature is generally much less, depending on details of the matter sector.

As in standard inflation, the value of H is not constant during inflation, but varies slowly, according to Eqs. (1) and (2). Each comoving wavenumber k passes through the horizon at a different time, so the scalar perturbations vary with scale, with a spectrum described by a spectral index n_S: $\Delta_S^2 \propto k^{n_S-1}$. In the spooky scenario, this "tilt" in the spectrum is given simply by

$$n_S - 1 \equiv \frac{d\ln\Delta_S^2}{d\ln k} = \frac{d\ln H}{d\ln k} = -\epsilon, \tag{24}$$

where ϵ denotes the standard slow roll parameter,

$$\epsilon \equiv (V'/V)^2(16\pi G)^{-1}. \tag{25}$$

Because $\Delta_S^2 \propto H$ and not H^2 (as is usual), the tilt differs by a factor of two from the standard relation[6]. Thus, constraints on the allowed potential shape also change: potentials preferred in the spooky scenario are strongly excluded for standard models, and *vice versa*.

Eqs. (24) and (25) imply that the measured tilt depends only on V'/V at the epoch when the measured range of scales passes through the horizon. The measured value [4, 5] $1 - n_S = 0.035 \pm 0.004$ constrains its logarithmic slope to be close to the inverse Planck mass:

$$\left(\frac{V'}{V}\right)_{\phi_0} = \frac{\sqrt{16\pi\epsilon}}{m_P} = 1.32 m_P^{-1}\left(\frac{1-n_S}{0.035}\right)^{1/2}. \tag{26}$$

As usual, sufficient inflation to reach the current scale of the universe requires $N \approx 60$ e-foldings since $\phi = \phi_0$, depending on reheating and subsequent evolution. In the slow roll approximation,

$$|\dot\phi/\phi|_{\phi_0} \approx H(\phi_0)/N. \tag{27}$$

Combination of Eqs. (1), (3), (26) and (27) leads to an absolute estimate of ϕ_0, independent of an assumed form for the potential:

$$\phi_0 \approx \frac{N}{8\pi}\left(\frac{V'}{V}\right)_{\phi_0} m_P^2 \approx 3.1\ m_P\ \frac{N}{60}\left(\frac{1-n_S}{0.035}\right)^{1/2}. \tag{28}$$

These results show that properties of the effective potential V in the exotic scenario are in principle overdetermined by measurements. The value and slope of the potential determine respectively the amplitude and spectral tilt of the relic perturbations. Given the tilt, the value of ϕ_0 determines the number of e-foldings— that is, the size of the currently observable universe.

It is not trivial for a potential to satisfy these experimental constraints on both N and n_S. For example, a potential of monomial form $V \propto \phi^b$ satisfies Eqs. (26) and (28) if and only if

$$b = \phi_0(V'/V)_{\phi_0} = 2N\epsilon = 4.1\ \frac{N}{60}\left(\frac{1-n_S}{0.035}\right), \tag{29}$$

so cosmological measurements agree (to within measurement errors) with $b = 4$, but not with other integer values. A potential of the form

$$V = \mathcal{V}\phi^4, \tag{30}$$

fits current measurements with $N = 59 \pm 7$, and a coefficient $\mathcal{V} \approx 10^{-20}$ in Planck units that depends on α, N and n_S. A potential of this form (Eq. 30) is now ruled out for standard inflation[6]. The range of viable models will be more constrained by improved measurements of the tilt.

B. Comparison with inflaton field fluctuations

In standard slow-roll inflation, scalar fluctuations $\Delta_{S,\delta\phi}$ from quantum fluctuations of the inflaton field (e.g. [7–9]) depend not only on H, but also on ϵ:

$$\Delta^2_{S,\delta\phi} = (H^2/2\pi\dot{\phi})^2 = \frac{1}{8\pi^2} H^2 t_P^2 \epsilon^{-1}. \quad (31)$$

These effective modes presumably still exist in the spooky system, but they are subdominant. Comparing Eq. (31) to Eq. (21), the exotic effect dominates for observationally viable values of ϵ and H in the spooky scenario:

$$\Delta^2_S/\Delta^2_{S,\delta\phi} = 8\pi^2\alpha\epsilon/H(\phi_0)t_P >> 1, \quad (32)$$

which validates the consistency of our approximation to neglect the gravitational effect of virtual inflaton fluctuations. The value of H is now so small that they are unimportant.

Similarly, the exotic scalar spectral index tilt (Eq. 24)— like the standard prediction for tensor tilt— depends only on ϵ, whereas the standard prediction, because it also depends on the second derivative of V, allows a larger variety of potentials that fit measurements. The running (change with scale) of the spectral index is predicted to be very small, as in many standard models.

C. Tensor perturbations

To agree with current Planck-sensitivity laboratory constraints[44], an exact symmetry is built into the models here (for example, in Eq. 4) such that spooky tensor-like correlation modes vanish. Because of the directional antisymmetry, perturbation multipoles are only odd; the even directional multipoles, including quadrupolar gravitational waves, vanish. As a result, tensor perturbations from spooky fluctuations are predicted to be small.

Of course, gravitational waves must still exist, but in emergent theories of gravity, gravitational waves, like curvature, are emergent rather than fundamental degrees of freedom[31–34]. The standard theory of a spin-2 graviton has a similar status to the theory of phonons— they are physically real, but are not fundamental quanta. Their quantum fluctuations should be described by the standard effective theory, linearized general relativity.

In the context of inflation, the usual quantum theory of tensor modes applies to these effective degrees of freedom. The metric can be quantized in the standard way by linearized quantum gravity, so tensor perturbations occur with the standard value, $\Delta^2_T = H^2 t_P^2/2\pi^2$. The exotic scenario thus predicts a tensor to scalar ratio

$$r = \Delta^2_T/\Delta^2_S = H t_P/2\pi^2\alpha = \Delta^2_S/2\pi^2\alpha^2, \quad (33)$$

which is far too small to measure. It is many orders of magnitude below the current experimental upper bound[3, 4], $r < 0.07$, and much smaller than predictions of some standard slow-roll inflation models (e.g. [45, 50]) that fit current data well[6] without spooky correlations.

D. Consistency of the Effective Potential

In standard inflation, a "super-Planckian" value of ϕ, as in Eq. (28), often leads to inconsistency from divergences in an effective field expansion[8, 9]. However, in an emergent space-time, this apparent difficulty could be an artifact of inappropriately applied quantum field degrees of freedom: classical space and time are separable only in systems much larger than the Planck length, and quantum field degrees of freedom are separable from space-time only well below the Planck mass. In this context, it is consistent to adopt a classical approximation for the unperturbed background geometry on the scale $H^{-1} >> t_P$ with any classical expectation value ϕ.

As in many inflation models, the exotic scenario does not address the physical origins of $V(\phi)$, or its connection with known matter fields. The one small number in the model (which can be taken as the coefficient $\mathcal{V}$ in Eq. (30)) is not explained.

IV. SIGNATURES OF SPOOKY CORRELATIONS

The last section showed that the power spectrum of perturbations in the spooky scenario agrees with standard concordance cosmology, and with current data. However, covariances significantly depart from standard predictions for some observables: unique spooky correlations among relic mode phases produce measurable statistical signatures in the distribution of matter and radiation at late times, that distinguish spooky models from standard inflationary fluctuations or latter-day classical processes.

The following considerations do not rely on specific features of the quantum models introduced above. As before, space-time in the classical era— above the shaded region in Fig. (1)— is described by a standard FRW background metric with linear curvature perturbations. The perturbations are required to obey the usual constraints that apply to any space-time, such as general covariance, as well as the standard global cosmological symmetries of homogeneity and isotropy. The new feature added by spooky inflation is to relax the usual constraints on locality of initial conditions. New kinds of spooky spacelike correlations permit phase correlations, among classical modes in different directions and on different scales, that are not possible in the standard picture. The new correlations are still highly constrained by cosmological symmetries, and must obey a new directional antisymmetry that is potentially observable. As

elaborated further in the Appendix, in a fully relational model of quantum gravity this classical relic statistical signature ultimately corresponds to an antisymmetry of relational quantum states similar to those studied above.

A. Classical perturbations

As above, assume a standard unperturbed classical background cosmology, including (unquantized) slow-roll inflation and the standard late-universe concordance model, ΛCDM. In linear perturbation theory[51], a gauge-invariant curvature perturbation $\Delta(\vec{x})$ is constant with time on a world line at fixed comoving coordinate $\vec{x}$. The transform in comoving wavenumber space $\vec{k}$ is:

$$\tilde{\Delta}(\vec{k}) = \int d\vec{x}\Delta(\vec{x})e^{i\vec{k}\cdot\vec{x}} = |\tilde{\Delta}(\vec{k})|e^{i\theta(\vec{k})}. \qquad (34)$$

For linear perturbations with only pressureless cold matter, both the modulus $|\tilde{\Delta}(\vec{k})|$ and phase $\theta(\vec{k})$ of modes are constant. Mean square curvature perturbations are given by integrals over the power spectrum Δ^2_S. As discussed above, in the real universe, perturbations are statistically isotropic, and close to scale invariant: $\Delta^2_S \propto |k|^{n_S-1}$, where n_S is close to 1.

On very large scales today, not only the power spectrum but also the actual distributions $\Delta(\vec{x})$ and $\tilde{\Delta}(\vec{k})$ are almost the same now as they were at the end of inflation. They are modified by a modest factor by radiation-pressure-driven movement of baryons before recombination, but even so, until they become nonlinear at late times, the comoving position of the bulk of the matter (that is, cold dark matter) in a large scale mode has moved only a small fraction of a wavelength from where it originated. We can say that primordial phases, still preserved in relic linear perturbations of density on large scales, "remember" the detailed pattern in comoving coordinates that was impressed by the process that formed them during inflation.

1. *Correlations of standard inflationary perturbations*

Cosmic perturbations in the standard picture arise from the gravitational effect of quantum fluctuations of the inflaton field around its expectation value, frozen in when they cross the horizon during inflation. In simple models based on gaussian fluctuations of a free quantum field, the phases and amplitudes of each mode are independent random variables set by an initial vacuum state. In this case, $\tilde{\Delta}^2_S(|k|)$ contains all the information that remains of the primordial process.

In a broad class of widely studied nongaussian models of locally-interacting fields during inflation, the $|\tilde{\Delta}(\vec{k})|$'s can be correlated with each other. The usual measure of correlations among modes is the bispectrum (*e.g.*, ref. [52]),

$$B(\vec{k}_a) = \langle\tilde{\Delta}(\vec{k}_1)\tilde{\Delta}(\vec{k}_2)\tilde{\Delta}(\vec{k}_3)\rangle, \qquad (35)$$

defined as an average of transforms $\tilde{\Delta}(\vec{k})$ for triplets of wave vectors $\vec{k}_a$ that contribute to the distribution. It is well known that for correlations from local field interactions, including nongaussian correlations of fields, the bispectrum is nonzero only for a closed triangle of wave vectors, $\sum_a \vec{k}_a = 0$. This property is associated with local momentum conservation for interactions. This broad class of nongaussian models has been tested using recent data[53].

We will now show that spooky correlations have distinctive properties that are cleanly distinguishable from any of these models. They have a gaussian distribution of amplitudes, but also spooky nonlocal and multidirectional phase correlations that cannot be produced by any local field theory on a classical background.

B. Spooky Perturbations

In the spooky model, the emergence from a quantum system of a classical geometry — an expanding universe with a local cosmic standard of rest— is inseparable from the formation of perturbations. Fluctuations in the process of emergence *are* the source of the perturbations.

Nonlocal collapse of the wave function— the projection of the quantum state onto an emergent observer's comoving frame— ensures that the states of nested causal diamonds are consistent. They entangle with each other to approximate a classical local inertial frame everywhere consistent with the global emergent metric.

The spooky correlations violate locality and local momentum conservation in a particular and highly constrained way. The physical process must still be generally covariant— it can only depend on quantities that do not depend on coordinates or a particular classical solution. Perturbations must also respect cosmological symmetries on all scales during the classical era after they leave the inflationary horizon— they must be statistically homogeneous and isotropic.

On the other hand, space and time are now slightly indeterminate on pre-emergent, sub-horizon scales, so local momentum conservation is no longer imposed by a classical metric (and a local inertial frame) on perturbations as they freeze in. Physically, this means that momentum and emergent time can be virtually "borrowed" and "paid back", on the scale of the horizon, among all the modes as they freeze out. It is not necessary for all correlations among non-coplanar modes to vanish, only that appropriately invariant averages do. The statistical properties of emergent spooky perturbations must depend only on covariant combinations of wave vectors.

1. General covariance, statistical isotropy, antisymmetry

Consider first the requirement of general covariance. Let u^ν_ϕ denote the 4-vector field defined by the timelike inflaton field gradient, and let $k^\kappa_1, k^\lambda_2, k^\mu_3$ denote a triplet of perturbation mode wave vectors in 3+1 dimensions. Using the antisymmetric Levi-Civita 4-tensor $\epsilon_{\kappa\lambda\mu\nu}$, define a covariant scalar projection,

$$\mathcal{E}_{4D} \propto \epsilon_{\kappa\lambda\mu\nu} k^\kappa_1 k^\lambda_2 k^\mu_3 u^\nu_\phi. \tag{36}$$

This expression is manifestly invariant under coordinate transformations for any triplet of wave vectors.

Now consider the spatial projection onto standard expanding comoving coordinates in 3D. As usual, the homogeneous background, encoded here in u^ν_ϕ, breaks boost invariance. In the cosmic comoving coordinate frame, $u^\nu_\phi \propto (1,0,0,0)$, so Eq. (36) projects onto surfaces of constant comoving proper time as a scalar triple product for each triplet of 3D $\vec{k}$'s:

$$\mathcal{E}(\vec{k}_1, \vec{k}_2, \vec{k}_3) \equiv \epsilon_{ijk} k^i_1 k^j_2 k^k_3 / k^3_0. \tag{37}$$

Geometrically, this dimensionless triple product represents the oriented volume of the parallelepiped defined by the $\vec{k}$'s. It vanishes when the $\vec{k}_a$'s lie in the same plane, so any closed triangle maps onto $\mathcal{E} = 0$. Up to a choice of normalization scale k_0, $\mathcal{E}$ represents a unique invariant number derived from a 3D comoving wave vector triplet. It is odd under spatial reflections, $\vec{k} \to -\vec{k}$.

This projection shows that it is possible to produce a scalar distribution in comoving space that is generally covariant, statistically isotropic, and directionally antisymmetric. For this to happen, is necessary to abandon the constraint of local momentum conservation that requires coplanar momenta.

The directional antisymmetry can be traced to how locality arises in an emergent system, where positions in relation to an observer arise from directional quantum operators, rather than a fixed background. In this kind of system, the odd parity of 3D spatial projections of directional relationships onto comoving 3-space by the inflationary horizon is a generic behavior that largely follows from classical covariance. Since a three dimensional space is spanned by three basis vectors, and the scalar product of three non-coplanar vectors is antisymmetric, an emergent scalar with zero mean, such as a spooky curvature perturbation, is naturally odd under reflections and vanishes at the origin,

$$\Delta(\vec{x}) = -\Delta(-\vec{x}) \quad \text{and} \quad \tilde{\Delta}(\vec{k}) = -\tilde{\Delta}(-\vec{k}). \tag{38}$$

Physically, the antisymmetry arises from a simultaneous antisymmetric "collapse" of the wave function at horizon antipodes, as the classical comoving frame forms on the inflationary horizon. The same projection properties are familiar in angular momentum, such as those in the quantum spin algebra discussed previously.

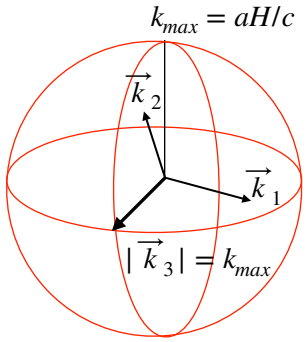

FIG. 8. Timing of freezing or collapse of entangled mode states in comoving $\vec{k}$ space. A triplet of comoving wave vectors is shown at a time when the largest of them, the last of the triplet to freeze out, matches the inflationary horizon, that is, when it "becomes classical" at $|\vec{k}| = aH/c$. Smaller values of k will have frozen earlier into classical perturbations. In the spooky scenario, wave vectors with $|\vec{k}| > aH/c$ are still indeterminate, with entangled spatial directions.

2. Measures of scale-invariant antisymmetry

Antisymmetric projections can be used to define global statistical measures of spooky nonlocal multidirectional correlations that emerge in classical perturbations. For a spooky inflation, the most useful projections are scale-invariant: the normalization k_0 for each triplet has a value such that $\mathcal{E}$ only depends on the shape of the parallelepiped, not on its absolute scale.

The simplest covariant, scale-invariant normalization choice for $\mathcal{E}$ is $k^3_0 = |\epsilon_{ijk} k^i_1 k^j_2 k^k_3|$:

$$\mathcal{E}_0(\vec{k}_1, \vec{k}_2, \vec{k}_3) \equiv \epsilon_{ijk} k^i_1 k^j_2 k^k_3 / |\epsilon_{ijk} k^i_1 k^j_2 k^k_3|. \tag{39}$$

With this choice, $\mathcal{E}_0 = \pm 1$ for all non-coplanar triplets; it just measures their parity.

The parity projection (Eq. 39) does not differentiate correlations among modes of different scales. Other scale-invariant normalizations are possible that allow spatial filtering. They offer several advantages: measurements over limited ranges of $|\vec{k}|$; measurement of correlations among scales that freeze out at different times; and explicit tests of scale invariance.

One such projection is motivated by a simplified physical picture, shown in Fig. (8). During inflation, the initial conditions for classical mode correlations are determined physically as entangled states in three spatial directions freeze into classical modes. In this view, the state of each mode when it freezes is drawn from a distribution determined by the states of already-frozen modes with smaller $|k|$ in all directions. The ongoing collapse of the quantum system ends when the smallest comoving scale freezes in, when the apparent horizon disappears at the end of inflation— the end of the null quantum region

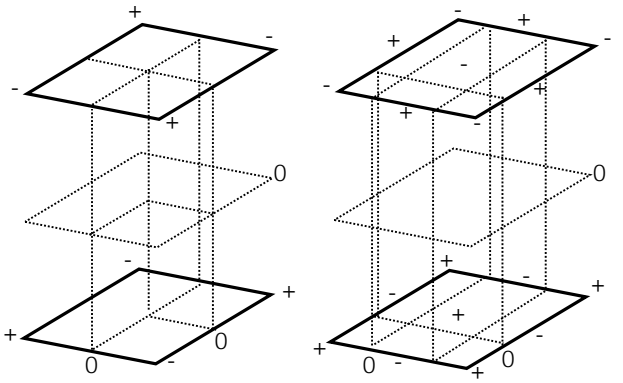

FIG. 9. Exploded view in 3-space of cells showing maxima, minima, and zeros of the two types of rectilinear antisymmetric triplet eigenmodes (Eq. 43), for an observer at the center. Some spatial planes of zeros are shown as dotted lines.

boundary in Fig. (1). Over the measured astronomical range of scales, this process is approximately scale-free, and the same should be true of frozen correlations among modes.

A physically natural scale-invariant normalization for the projection $\mathcal{E}$ is thus the magnitude of the last mode of each triplet to freeze out,

$$\mathcal{E}(\vec{k}_1, \vec{k}_2, \vec{k}_3) = \epsilon_{ijk} k_1^i k_2^j k_3^k / k_{max}^3, \tag{40}$$

where

$$k_{max} \equiv \max[|\vec{k}_1|, |\vec{k}_2|, |\vec{k}_3|], \tag{41}$$

as illustrated in Fig. (8). In this case, $\mathcal{E}$ takes values -1 or 1 when the $\vec{k}$'s are orthogonal with equal lengths, and lies between these values if any of the $|k_j|$'s differ. This normalization distinguishes the shape as well as parity of the oriented parellepiped defined by the vector triplet, so it allows scale-free statistical measures of the entanglement between different scales as well as different directions. The discussion below assumes a scale-invariant definition of $\mathcal{E}$, of which Eq. (40) is one example. The normalization in Eq. (40) also allows spatial filtering with just a single scale, which will be used below for practical spookiness estimators.

In the place of Eq. (35), a new kind of antisymmetric bispectrum can be defined using the invariant antisymmetric projection $\mathcal{E}(\vec{k}_1, \vec{k}_2, \vec{k}_3)$:

$$\mathcal{B} = \langle \mathcal{E}(\vec{k}_1, \vec{k}_2, \vec{k}_3)\ \tilde{\Delta}(\vec{k}_1)\tilde{\Delta}(\vec{k}_2)\tilde{\Delta}(\vec{k}_3)\rangle. \tag{42}$$

It measures correlations of Δ that are odd under reflections. It is only nonzero for non-coplanar triplets of wave vectors, so it vanishes in standard theories; it is the simplest example of a measure of "spookiness" in the distribution.

3. Spooky realizations

Odd-parity distributions can clearly be realized mathematically by construction. Instead of a general decomposition into independent plane waves (Eq. 34), an odd distribution can be written as a sum of odd-parity 3D triplet modes that depend jointly on entangled states in three spatial directions:

$$\Delta(\vec{x}) = \sum_{\vec{k}_1,\vec{k}_2,\vec{k}_3} \alpha(\vec{k}_1, \vec{k}_2, \vec{k}_3) \sin(\vec{k}_1 \cdot \vec{x}) \sin(\vec{k}_2 \cdot \vec{x}) \sin(\vec{k}_3 \cdot \vec{x}) + \beta(\vec{k}_1, \vec{k}_2, \vec{k}_3) \sin(\vec{k}_1 \cdot \vec{x}) \cos(\vec{k}_2 \cdot \vec{x}) \cos(\vec{k}_3 \cdot \vec{x}). \tag{43}$$

The second row terms are odd under reflection through the origin but even on reflection in the plane determined by $\vec{k}_2$ and $\vec{k}_3$. They single out a direction on each scale, but the overall distribution is statistically isotropic when averaged over all scales.

The spatial layouts of maxima and minima for odd 3D rectilinear triplet modes are shown in Fig. (9). In general, an odd 3D triplet mode can have different values of wave numbers along the three directions. A spooky odd-parity cosmological distribution is in general composed of a superposition of such 3D triplet modes, allowing different orientations on different scales. The previous analysis shows that the overall distribution can be statistically isotropic, homogeneous and scale invariant, if the distributions of α and β are functions only of the combination $\mathcal{E}(\vec{k}_1, \vec{k}_2, \vec{k}_3)$.

A particular triplet decomposition (Eq. 43) is not invariant, but is unique to a particular observer, the origin of coordinates (although any given triplet will apply to a discrete set of periodically-spaced observers). Since the spatial distribution always vanishes at the origin of coordinates, it should be interpreted physically as a realization of time distortion or curvature relative to a freely falling geodesic at the origin, not relative to a globally defined, unperturbed classical background. This assignment of a relational observable quantity is in keeping with the emergent character of the whole metric. In our set-up where a horizon is a quantum object, there is no universal, determinate "true" background metric, only one defined in relation to a particular observer and its particular inflationary horizon. The odd parity is a remnant of primordial nonlocal correlations that freeze in at spacelike separation from any observer, on its horizon.

Here then is frozen quantum weirdness on the largest scales: every observer ends inflation with zero total local perturbation. Every observer has a different horizon, so the zero point of the potential is observer-dependent; on the other hand, all observers agree on measurable quantities, such as differences in $\Delta(\vec{x})$ between world lines in a realized classical distribution over a region where they can compare measurements. There is no inconsistency

between observers because there is no way to tell "who is right" about an absolute cosmic background frame. Different observers look at different but entangled quantum mechanical subsystems that have collapsed into the same classical state where they overlap.

4. Generic signature of spooky inflation

Of course, the interesting physical question remains whether such weird correlations are actually produced during inflation. Fortunately, this question may be answered by measurement. If spooky perturbations are the dominant source of primordial perturbations, the exotic antisymmetric correlation power is a substantial fraction of the total perturbation, so primordial curvature perturbations are expected to show a large effect,

$$\langle \mathcal{B}^2 \rangle \approx \langle \Delta^2 \rangle^3. \tag{44}$$

For standard field-mode perturbations, the opposite is true: correlations between modes can only exist for coplanar wave vectors, for which $\mathcal{E} = 0$, so the antisymmetric phase power is predicted to identically vanish:

$$\mathcal{B} = 0. \tag{45}$$

Thus, a detection of $\mathcal{B} \neq 0$ can in principle provide a model-independent signature of spooky primordial phase correlations.

5. Antisymmetric spookiness estimators

We now turn to practical measures of spookiness detectable in cosmic structure. In the projection of the quantum state vector onto the outgoing space, the choice of observer defines the measurement. The triplet mode decomposition in Eq. (43) displays exact antisymmetry in all modes around only one point, the observer. On the other hand, there is a statistical tendency everywhere towards odd correlations, which becomes conspicuous by convolving the distribution with an antisymmetric kernel. This property should allow the spookiness of relic correlations in the actual universe to be estimated from cosmic surveys.

A realistic estimator of correlations can be designed with a response that optimizes the power of a measurement in a particular situation. One approach is to use antisymmetric wavelets $\mathcal{W}_L$ that probe spooky correlations mainly on scale L, with transforms shaped to have relatively little response to $k_{max} >> 1/L$. To search for the spooky effect, and to differentiate it from standard perturbations, it is not necessary for the wavelets to match the exact pattern of primordial correlation; it is sufficient that a suitable convolution of $\mathcal{W}_L$ with Δ responds to significant fluctuation power with $\mathcal{B} \neq 0$.

The convolution is most easily written as a product in transform space. The normalized spookiness $\mathcal{S}$ of a distribution $\Delta(\vec{x})$ on scale L can be defined via a normalized wavelet-dependent functional similar to $\mathcal{B}$,

$$\mathcal{S}[\mathcal{W}_L] \equiv \langle \tilde{\mathcal{W}}_L(\mathcal{E})\ \tilde{\Delta}(\vec{k}_1)\tilde{\Delta}(\vec{k}_2)\tilde{\Delta}(\vec{k}_3)\rangle\ \langle \tilde{\Delta}_L^2\rangle^{-3/2}, \tag{46}$$

where $\tilde{\mathcal{W}}_L(\mathcal{E})$ is an odd function of the scale-invariant combination $\mathcal{E}(\vec{k}_1, \vec{k}_2, \vec{k}_3)$, with a filtering scale L imposed via a UV cutoff for each triplet at about $k_{max} \approx 1/L$. Again, for standard perturbations, the spookiness vanishes, because the $\tilde{\Delta}(\vec{k})$'s are symmetric.

A simple choice in transform space $\tilde{\mathcal{W}}_L$ would be a filtered antisymmetric spectrum linear in $\mathcal{E}$,

$$\begin{aligned} \tilde{\mathcal{W}}_L &= \mathcal{E}, \qquad k_{max} < 1/L, \\ &= 0, \qquad k_{max} > 1/L, \end{aligned} \tag{47}$$

with some suitable scale-invariant normalization for $\mathcal{E}$, such as Eq. (40). In configuration space, antisymmetric wavelets can be constructed from normalized sums of odd triplet modes as in Eq. (43),

$$\begin{aligned} \mathcal{W}_L = \sum_{\vec{k}_1,\vec{k}_2,\vec{k}_3}^{k<k_{max}(L)} & \alpha_{\mathcal{W}}(\mathcal{E}) \sin(\vec{k}_1\cdot\vec{x}) \sin(\vec{k}_2\cdot\vec{x}) \sin(\vec{k}_3\cdot\vec{x}) \\ & + \beta_{\mathcal{W}}(\mathcal{E}) \sin(\vec{k}_1\cdot\vec{x}) \cos(\vec{k}_2\cdot\vec{x}) \cos(\vec{k}_3\cdot\vec{x}). \end{aligned} \tag{48}$$

For example, a simple two-parameter wavelet can be designed by choosing $\alpha_{\mathcal{W}} \propto \mathcal{E}$ and $\beta_{\mathcal{W}} \propto \mathcal{E}$.

The value of $\mathcal{S}$ depends on how well the structure of the wavelet matches that of $\tilde{\Delta}(\vec{x})$. If spooky perturbations dominate the spectrum, a normalized antisymmetric wavelet $\mathcal{W}_L$ well matched to the primordial structure yields $\mathcal{S}$ of order unity.

By not averaging over one of the wave vectors, one can define a measure of the overall asymmetry of the filtered distribution, associated with a specific direction and scale defined by a wave vector $\vec{k}_D$:

$$\mathcal{D}_L(\vec{k}_D) = \langle \tilde{\mathcal{W}}_L(\vec{k}_D, \vec{k}_2, \vec{k}_3)\tilde{\Delta}(\vec{k}_D)\tilde{\Delta}(\vec{k}_2)\tilde{\Delta}(\vec{k}_3)\rangle_{\vec{k}_2,\vec{k}_3} \tag{49}$$

On any given scale $|\vec{k}_D|$, the directional map $\mathcal{D}_L(\vec{k}_D)$ has an angular distribution given by a sum of only odd-parity spherical harmonics, $\ell = 1, 3, 5 \ldots$. Its dipole ($\ell = 1$) mode defines a preferred axis and direction, frozen in at the time when that scale froze out, $aH/c \approx |\vec{k}_D|$.

A particular realization breaks directional and translational symmetry on each scale. On any smoothing scale L, there is a dipole component with a principal axis on any larger length scale, defined from Eq. 49, with an origin-dependent spatial phase. However, the mean dipole of the distribution vanishes when averaged over all of space because its direction changes sign from place to place, and the system as a whole is statistically isotropic,

because the principal correlation axis varies with scale. The radial and angular correlations among odd directional multipoles, and correlations between principal correlation axes at different places, depend on how freezing on the inflationary horizon correlates structures over a range of time. Principal axes for nearby world lines (closer than $\approx 1/|\vec{k}_D|$) tend to be aligned, and multipole components around each world line are correlated with each other.

V. MEASUREMENT IN COSMIC SURVEYS

A. Cosmic Microwave Background Anomalies

The pattern of CMB temperature anisotropy on large angular scales has long been known to display several surprising "anomalies"[54, 55] that are often dismissed as insignificant flukes. We now suggest that some of them can instead be naturally attributed to spooky inflationary correlations, even though the perturbation power spectrum is the same as standard ΛCDM cosmology. The large angle anisotropy approximates a particularly simple projection that preserves the antisymmetry of primordial perturbations, so general arguments can demonstrate specifically how new spooky covariances modify standard predictions.

As shown above (Eq. 38), spooky inflation predicts directional antisymmetry of $\Delta(\vec{x})$ around any observer. The CMB temperature perturbation $\delta T/T$ smoothed on large angular scales is approximately proportional to the primordial distribution $\Delta(\vec{x})$ on a sphere, the cosmic last scattering surface. Thus to a first approximation, the spherical-harmonic decomposition of temperature anisotropy at low angular wavenumbers ℓ should be exactly directionally antisymmetric. The fluctuation band power (TT) should have approximately twice the noise power usually expected in odd spherical harmonics $\ell = 1, 3, \ldots$, and a small fraction of the usual power in even harmonics $\ell = 2, 4 \ldots$ (This odd/even anomaly is not expected to appear in temperature-polarization (TE) correlation, since polarization is generated physically by an even-parity quadrupole, so it starts spatially out of phase with T and Δ.) Although the intrinsic dipole ($\ell = 1$) is predicted to be larger than usually expected, it is not measured, because it cannot be separated from the much-larger-still local kinematic dipole. Since the quadrupole ($\ell = 2$) amplitude is predicted to be negligible compared with its usually expected value, the octopole ($\ell = 3$) modes are the lowest harmonics predicted to contribute appreciable observable anisotropy.

This simple prediction appears to be confirmed: a highly suppressed quadrupole and prominent octopole modes are well-established features in the TT bandpower spectrum[54, 55]. The same effect manifests as another well-established anomaly, a remarkably small two-point correlation function of $\delta T/T$ at large angular separation[55, 56]. In the spooky scenario, the dipole subtraction is predicted to remove almost all of the fluctuation power on angular scales larger than the octopole.

The odd/even effect is found to extend well beyond the lowest multipoles: it has been estimated[54, 55] that a statistically anomalous excess fluctuation power in odd multipoles extends up to about $\ell \approx 30$. This also agrees with a simple estimate of the expectation from primordial antisymmetry: at about this angular scale, the temperature anisotropy is significantly modified from its primordial antisymmetric pattern by waves in the recombination plasma.

The observed CMB temperature perturbation comes from perturbations in both radiation temperature and gravitational redshift. On scales much larger than the horizon at recombination, both effects preserve their primordial phase, and they tend to cancel each other. On smaller scales, propagating acoustic waves of baryon/photon plasma change the phase of the radiation temperature relative to the dark-matter-dominated potential. On scales where the effects reinforce each other, they form the well-known baryon acoustic oscillation peaks in the angular band power spectrum, the first of which peaks at $\ell \approx 100$. The symmetric baryon-photon waves should erase primordial antisymmetry above the scale where the red wing of this first acoustic peak matches the average large-angle temperature anisotropy band power. This occurs at about $\ell \approx 30$, the scale where parity asymmetry is indeed found to diminish[55].

As seen above, the multipole directions in spooky inflation are not independent. Spooky directional correlations could also naturally produce octopolar planarity, and alignments among normally-uncorrelated multipole components, as observed[55].

More rigorous comparisons with measurements are possible, by using standard linear theory for the post-inflation evolution including baryon and radiation transport, and customizing statistical tests to spooky predictions. The relatively small number of independent modes on large scales limits the statistical power of large angle TT anisotropy to test models—the p-values of the anomalies just described are typically at the percent level, and in the best cases about ten times smaller[55]— but more powerful tests of this interpretation might be possible as data improve on large angle polarization[57, 58].

B. Spooky correlations in galaxy surveys

1. *Advantages of 3D surveys*

Large-angle CMB anomalies hint that spooky primordial correlations may indeed have an antisymmetric structure. If so, the idea can in principle be tested with

3D surveys of cosmic structure, which have more information and statistical power than CMB surveys. They contain many more modes, since they can measure linear primordial correlations in a large 3D volume, on scales much smaller than the horizon.

In addition, 3D density structure preserves primordial phase information over a wider range of scales than CMB temperature does. As noted above, primordial perturbations even in the linear regime are modified by an early nongravitational effect: the acoustic propagation of baryon-photon waves before recombination shifts the phase of baryon density modes, and symmetrically randomizes their phases on scales up to approximately the horizon scale at recombination, effectively erasing TT antisymmetry. Since the the baryons constitute only about a fifth of the total matter density, the baryonic oscillations have a relatively small effect on the primordial spatial distribution of the potential. They are neglected in the rough estimate given here of survey sensitivity.

2. *Spookiness estimators based on linear density contrast*

A survey of galaxies or gas provides an estimate of mass density $\rho(\vec{x})$ when convolved over some kernel with a smoothing scale L. In the linear regime, the density contrast $\delta\rho(\vec{x}) \equiv \rho(\vec{x}) - \langle\rho\rangle$ is proportional to $\Delta(\vec{x})$ with the same kernel, with a linear coefficient that depends on L:

$$(\delta\rho(\vec{x})/\langle\rho\rangle)_L \approx -\Delta_L(\vec{x})(L_H/L)^2, \tag{50}$$

where L_H denotes the Hubble scale, ≈ 4000Mpc in the present universe.

In the linear regime, the perturbation in potential is approximately constant with time on each scale. While the density contrast is not constant, the primordial pattern in comoving space is approximately preserved, until the density perturbation becomes nonlinear. A 3D galaxy survey thus allows a spookiness estimator similar to Eq. (46), based on density contrast:

$$\mathcal{S}_L = \langle\tilde{\mathcal{W}}_L(\mathcal{E})\tilde{\delta\rho}(\vec{k}_1)\tilde{\delta\rho}(\vec{k}_2)\tilde{\delta\rho}(\vec{k}_3)\rangle\ \langle\tilde{\delta\rho}_L^{\,2}\rangle^{-3/2}. \tag{51}$$

Because all standard models predict directional symmetry, a directionally antisymmetric wavelet $\tilde{\mathcal{W}}_L$, filtered at $k_{max} \approx 1/L$ for any smoothing scale L, provides a model-independent spookiness test. If the wavelet is well matched to the structure of dominant spooky correlations, $\mathcal{S}_L = \mathcal{O}(1)$; for standard perturbations, $\mathcal{S}_L = 0$.

3. *Estimate of survey requirements*

The next question is whether imperfect measurements of the linear density field can in principle show evidence of $\mathcal{S}_L \neq 0$, and hence signify $\mathcal{B} \neq 0$ in primordial fluctuations. The intrinsic limit of sensitivity for many finite-volume realizations with the same correlations can be written as an estimation noise error,

$$\delta\mathcal{S} \equiv \sqrt{\langle(\mathcal{S}_{estimated} - \mathcal{S}_{true})^2\rangle_{realizations}}, \tag{52}$$

where $\mathcal{S}_{true}$ refers to the spookiness of the "true" primordial comoving linear density field. For a wavelet optimally matched to the spooky structure, $\delta\mathcal{S}^{-1}$ gives an estimate of the best possible significance of a detection.

Even with an optimal sampling wavelet, there are unavoidable noise sources that contribute to $\delta\mathcal{S}$: nonlinear physical effects associated with galaxy formation that change the mapping of $\Delta(\vec{x})$ to galaxy density on small scales, and $\sqrt{N}$ noise in measurements of density from a limited sample. We will use order-of-magnitude estimates of these noise sources as a rough guide to estimate maximum survey sensitivity.

On small length scales where clustering is nonlinear, movement of matter smears out the one-to-one mapping between primordial potential perturbation and matter distribution: the antisymmetry of the primordial pattern gets mixed away on a gravitational timescale by nonlinear dynamics of orbital motions. As a result, most of the cleanly recoverable primordial phase information comes from a scale somewhat but not too much larger than the scale where density perturbations become nonlinear—roughly the scale of visible structures of the cosmic web, such as voids, pancakes and filaments.

Let L_* denote the smallest scale where the primordial pattern of curvature perturbations is mostly intact. Density contrast has unit variance in ≈ 20 Mpc diameter spheres, so for rough estimation we adopt a scale about twice as large, $L_* \approx 40$ Mpc, or $L_*/L_H \approx 10^{-2}$.

Nonlinear variations on scale L_* add noise to measurements on larger scales. White-noise density variance in a volume of size $L > L_*$ scales roughly like $(L_*/L)^3$, so the spookiness measurement noise on scale L,

$$\delta\mathcal{S}_L \approx (L_*/L)^{3/2}\langle(\delta\rho/\rho)^2\rangle_L^{-1/2} \approx (L/L_*)^{1/2}, \tag{53}$$

is always greater than unity in a single L-size volume. The primordial pattern in this sense is fundamentally buried in noise.

Even so, in principle a coherent spookiness signal can be still be extracted a large survey volume L_S^3 with about $(L_S/L)^3$ samples on scale L; the maximum signal to noise ratio scales like

$$[\delta\mathcal{S}^{-1}] \approx (L_S/L)^{3/2}(L_*/L)^{1/2} \approx (L_*/L)^2(L_S/L_*)^{3/2}. \tag{54}$$

This estimate accounts only for the purely "geometrical noise"— the information limit imposed by nonlinear structure. It errs on the optimistic side: it is the best one could hope for, if the primordial signal is maximally conspicuous and minimally contaminated.

One straightforward conclusion is that the mean square sensitivity is at most the number of effective voxels in the survey volume: $[\delta\mathcal{S}^{-2}]_{max} < (L_S/L_*)^3$. Thus, the survey should have the largest volume possible, $L_S \approx L_H$.

The steep dependence $\propto L^{-2}$ in Eq. (54) shows that most of the signal comes from the smallest measured structures where the primordial phase survives— both because there are more structures (or modes), and because the measured quantity, density contrast, is larger on small scales. For optimal sensitivity, the map of density structure should resolve the nonlinear clustering scale L_*. Expressed in terms of redshift $\delta z \equiv \delta LH/c$, ideally the resolution in all three dimensions should be better than $\delta z \approx L_*/L_H \approx 10^{-2}$. The maximum possible signal to noise ratio degrades quickly if the resolution is poor:

$$[\delta\mathcal{S}^{-1}]_{max} \approx 1000(10^2\delta z)^{-2}. \quad (55)$$

In addition to the survey volume and resolution requirements, there must be enough galaxies so that the sampling-noise contribution to the measurement error $\delta\mathcal{S}$ is less than the geometrical noise. Resolving the phase relationships of perturbations in 3D requires at least an order of magnitude more galaxies than simply measuring the direction-averaged power spectrum, which has been the design goal of most surveys to date. Guessing that measurement of a dipolar density wavelet fit in three dimensions requires at least a few galaxies along each direction in each L_* volume, or perhaps 10^2 galaxies, the total number of galaxies N in a Hubble-volume survey must be more than about

$$N \approx 10^2(L_H/L_*)^3 \approx 10^8. \quad (56)$$

With more galaxies, finer details of the primordial correlations can be resolved. Galaxy-sampling noise scales with L in the same way as the geometrical noise, so this requirement is approximately independent of L.

The optimal sensitivity estimate (Eq. 55) is promising enough to warrant more study with simulated realizations of surveys and estimators. A comparison between realizations with random initial phases, and realizations with spooky initial perturbations, can model and bound effects such as nonlinear clustering, numerical artifacts, survey geometry, sample selection, and nonuniform radial resolution.

4. Implementation in Real Surveys

The current dataset that comes closest to satisfying the above requirements is the Dark Energy Survey (DES)[59]. It includes more than 10^8 galaxies spread over about a Hubble volume as required; however, as it is a broad band photometric survey, it does not achieve $\delta z_* = 10^{-2}$ in the radial direction for the bulk of its galaxies[60]. Even allowing for this and additional numerical factors that may reduce overall significance by more than an order of magnitude below the value in Eq. (55), it is plausible that DES might achieve $\delta\mathcal{S} << 1$— that is, good enough for a detection if $|\mathcal{S}| = \mathcal{O}(1)$. DES may be the first survey capable of discovering spookiness at high significance.

Detailed studies of spookiness would place demands on surveys beyond design goals of existing and planned projects; the expanded scope could motivate extensions and possibly new surveys. In the future, LSST[61] will improve on DES in all respects, but will still not achieve optimal 3D resolution and sampling. An optimal survey would need good redshift precision, $\delta z < 10^{-2}$, in a Hubble-volume, densely sampled survey, with $N \approx 10^9$ galaxies. The largest volumes may some day be mapped at sufficient resolution using line emission from gas that is not resolved into galaxies.

VI. SUMMARY

Nonlocal, holographic, entangled states on the inflationary horizon, similar to those invoked to resolve black hole information paradoxes, can produce correlations in relic perturbations observably different from standard inflation models. Many of their properties are fixed by a single scale, the inflation rate H in Planck units, and well known symmetries of the emergent classical background.

The simplest generic consequence of spooky inflation is a nearly scale free spectrum of curvature perturbations, with an amplitude $\Delta^2 \approx Ht_P$ significantly larger than those associated with inflaton field fluctuations. Application of standard inflation theory with current measurements then yields direct constraints on the value of H and the slope of the effective potential. The shape of the effective potential is constrained to be close to $V(\phi) \propto \phi^4$ in the range of k observed, with a definite inflaton value several times the Planck mass. These parameters for the potential are ruled out in standard inflation[6]. Primordial tensor perturbations are predicted to be very small, based both on general symmetry arguments, and on existing Planck-sensitivity laboratory constraints.

Another distinctive and robust new prediction, in the sense of being insensitive to the details of specific spooky models, is an exact directional antisymmetry of the primordial distribution of curvature perturbations, traceable directly to the nonlocality and directional anticorrelation of initial conditions on the horizon, which is forbidden in standard models. Although the gaussian distribution and predicted evolution of the linear power spectrum are unchanged from the standard ΛCDM late time cosmological model, primordial antisymmetry will change covariances for some observables, modifying estimates of cosmological parameters and tests of consistency.

Signatures of primordial antisymmetry already appear

to be measured in CMB anisotropy, and if they are indeed due to nearly-scale-invariant primordial spookiness, they should also be observable in large scale 3D galaxy surveys, possibly even in existing data. Evidence for spooky correlations could signify a dominant role for new Planck scale quantum degrees of freedom in creating cosmic structure, and lead to empirical studies of emergent quantum gravity.

This work was supported by the Department of Energy at Fermilab under Contract No. DE-AC02-07CH11359.

[1] P. A. R. Ade *et al.* (Planck), Astron. Astrophys. **594**, A13 (2016).
[2] P. A. R. Ade *et al.* (Planck), Astron. Astrophys. **594**, A20 (2016).
[3] P. A. R. Ade *et al.* (BICEP2, Keck Array), Phys. Rev. Lett. **116**, 031302 (2016).
[4] Y. Akrami *et al.* (Planck), (2018), arXiv:1807.06205 [astro-ph.CO].
[5] N. Aghanim *et al.* (Planck), (2018), arXiv:1807.06209 [astro-ph.CO].
[6] Y. Akrami *et al.* (Planck), (2018), arXiv:1807.06211 [astro-ph.CO].
[7] K. Kadota, S. Dodelson, W. Hu, and E. D. Stewart, Phys. Rev. **D72**, 023510 (2005).
[8] D. Baumann, in *Physics of the large and the small, TASI 09* (2011) pp. 523–686, arXiv:0907.5424 [hep-th].
[9] M. Kamionkowski and E. D. Kovetz, Ann. Rev. Astron. Astrophys. **54**, 227 (2016).
[10] G. 't Hooft, (2016), arXiv:1605.05119 [gr-qc].
[11] G. 't Hooft, Found. Phys. **46**, 1185 (2016), arXiv:1601.03447 [gr-qc].
[12] G. 't Hooft, Foundations of Physics **48**, 1134 (2018).
[13] C. J. Hogan, Phys. Rev. D **95**, 104050 (2017).
[14] C. J. Hogan, O. Kwon, and J. Richardson, Class. Quantum Grav. **34**, 135006 (2017).
[15] C. Hogan and O. Kwon, Classical and Quantum Gravity **35**, 204001 (2018).
[16] C. Rovelli, *Quantum Gravity* (Cambridge University Press, 2004).
[17] C. Rovelli, Classical and Quantum Gravity **28**, 153002 (2011).
[18] T. Banks and W. Fischler, (2018), arXiv:1810.01671 [hep-th].
[19] J. D. Bekenstein, Phys. Rev. **D7**, 2333 (1973).
[20] S. Hawking, Commun. Math. Phys. **43**, 199 (1975).
[21] R. M. Wald, Living Rev. Rel. **4**, 6 (2001).
[22] G. 't Hooft, *Conference on Highlights of Particle and Condensed Matter Physics (SALAMFEST) Trieste, Italy, March 8-12, 1993*, Conf. Proc. **C930308**, 284 (1993).
[23] L. Susskind, J. Math. Phys. **36**, 6377 (1995).
[24] R. Bousso, Rev.Mod.Phys. **74**, 825 (2002).
[25] W. G. Unruh and R. M. Wald, Reports on Progress in Physics **80**, 092002 (2017).
[26] A. G. Cohen, D. B. Kaplan, and A. E. Nelson, Phys. Rev. Lett. **82**, 4971 (1999).
[27] S. Ryu and T. Takayanagi, Phys. Rev. Lett. **96**, 181602 (2006).
[28] S. Ryu and T. Takayanagi, JHEP **08**, 045 (2006).
[29] S. N. Solodukhin, Living Rev. Rel. **14**, 8 (2011).
[30] M. Natsuume, Lect. Notes Phys. **903**, pp.1 (2015).
[31] T. Jacobson, Phys. Rev. Lett. **75**, 1260 (1995).
[32] E. Verlinde, JHEP **1104**, 029 (2011).
[33] T. Padmanabhan, Gen. Rel. Grav. **46**, 1673 (2014).
[34] T. Jacobson, Phys. Rev. Lett. **116**, 201101 (2016).
[35] J. A. Wheeler, Proceedings of the American Philosophical Society **90**, 36 (1946).
[36] A. Zeilinger, Rev. Mod. Phys. **71**, S288 (1999).
[37] J. Handsteiner *et al.*, Phys. Rev. Lett. **118**, 060401 (2017), arXiv:1611.06985 [quant-ph].
[38] C. J. Hogan, Phys. Rev. **D85**, 064007 (2012).
[39] A. Chou, H. Glass, H. R. Gustafson, C. J. Hogan, B. L. Kamai, O. Kwon, R. Lanza, L. McCuller, S. S. Meyer, J. Richardson, C. Stoughton, R. Tomlin, and R. Weiss (Holometer Collaboration), Class. Quantum Grav. **34**, 065005 (2017).
[40] I. Ruo Berchera, I. P. Degiovanni, S. Olivares, and M. Genovese, Physical Review Letters **110**, 213601 (2013).
[41] I. Ruo-Berchera, I. P. Degiovanni, S. Olivares, N. Samantaray, P. Traina, and M. Genovese, Phys. Rev. A **92**, 053821 (2015).
[42] S. T. Pradyumna *et al.*, (2018), arXiv:1810.13386 [quant-ph].
[43] A. S. Chou, R. Gustafson, C. Hogan, B. Kamai, O. Kwon, R. Lanza, L. McCuller, S. S. Meyer, J. Richardson, C. Stoughton, R. Tomlin, S. Waldman, and R. Weiss (Holometer Collaboration), Phys. Rev. Lett. **117**, 111102 (2016).
[44] A. Chou, H. Glass, H. R. Gustafson, C. J. Hogan, B. L. Kamai, O. Kwon, R. Lanza, L. McCuller, S. S. Meyer, J. Richardson, C. Stoughton, R. Tomlin, and R. Weiss (Holometer Collaboration), Class. Quant. Grav. **34**, 165005 (2017).
[45] A. Starobinsky, Physics Letters B **91**, 99 (1980).
[46] C. J. Hogan, Phys. Rev. **D66**, 023521 (2002).
[47] C. J. Hogan, Phys. Rev. **D70**, 083521 (2004).
[48] C. J. Hogan, "A model of macroscopic geometrical uncertainty," (2012), arXiv:1204.5948 [gr-qc].
[49] Landau, L. D. and Lifshitz, E. M., *Quantum Mechanics: Non-Relativistic Theory* (Oxford: Pergamon, 1977).
[50] A. A. Starobinsky, Sov. Astron. Lett. **9**, 302 (1983).
[51] J. M. Bardeen, Phys. Rev. D **22**, 1882 (1980).
[52] J. M. Maldacena, JHEP **05**, 013 (2003), arXiv:astro-ph/0210603 [astro-ph].
[53] P. A. R. Ade *et al.* (Planck), Astron. Astrophys. **594**, A17 (2016).
[54] P. A. R. Ade *et al.* (Planck), Astron. Astrophys. **594**, A16 (2016), arXiv:1506.07135 [astro-ph.CO].
[55] D. J. Schwarz, C. J. Copi, D. Huterer, and G. D. Starkman, Class. Quant. Grav. **33**, 184001 (2016).
[56] C. J. Copi, D. Huterer, D. J. Schwarz, and G. D. Starkman, Mon. Not. Roy. Astron. Soc. **399**, 295 (2009), arXiv:0808.3767 [astro-ph].
[57] C. J. Copi, D. Huterer, D. J. Schwarz, and G. D. Starkman, Mon. Not. Roy. Astron. Soc. **434**, 3590 (2013), arXiv:1303.4786 [astro-ph.CO].
[58] A. Yoho, S. Aiola, C. J. Copi, A. Kosowsky, and G. D. Starkman, Phys. Rev. **D91**, 123504 (2015), arXiv:1503.05928 [astro-ph.CO].
[59] A. Drlica-Wagner *et al.* (DES), Astrophys. J. Suppl. **235**, 33 (2018), arXiv:1708.01531 [astro-ph.CO].

[60] B. Hoyle *et al.* (DES), Mon. Not. Roy. Astron. Soc. **478**, 592 (2018), arXiv:1708.01532 [astro-ph.CO].
[61] Z. Ivezic *et al.* (LSST), (2008), arXiv:0805.2366 [astro-ph].

VII. APPENDIX

Correlations of emergent proper time between separate world lines

The spooky inflation scenario is predicated on the idea that space-time emerges from a quantum system. Basic conceptual elements of classical space-time relationships, such as localized events and local inertial frames, are approximate, emergent properties of a quantum system with new, exotic correlations. Although there is no accepted theory of relational quantum gravity, some properties of the spooky correlations can be guessed from known causal symmetries of the classical space-time.

One model of quantum departure from classical behavior used to illustrate spooky correlations is the spin-algebra model of Eq. (4), which describes a nonlocal spatial antisymmetry of proper time displacement operators on the surfaces of causal diamonds. A simple extension of the model is sketched here to connect it with the relationship of proper time between separate world lines, encoded in the entanglement of their states. The relationship is encoded as pure entanglement information, in the form of an imaginary cross spectrum of time displacements.

Consider cross correlations between states of light cones on two world lines, A and B, that are classically at rest with respect to each other. Let $\hat{\delta}^{\pm}_{AB}$ and $\hat{\delta}^{\pm}_{BA}$ denote operators analogous to the raising and lowering operators $\hat{\delta}_{i\pm}$ (Eq. 12): single-quantum, Planck-scale projections, in the A and B rest frames, along the AB and BA spatial separation directions respectively. In addition to the spatial antisymmetry already established, they are also odd on reflection in time, depending on the orientation towards the past $(-)$ or future $(+)$:

$$\hat{\delta}^{+}_{AB} = -\hat{\delta}^{-}_{AB}. \tag{57}$$

These operators can be used to make a model of emergence: eigenvalues of $\hat{\delta}^{\pm}_{AB}$, $\hat{\delta}^{\pm}_{BA}$ represent projections, on each world line, of states on a discrete Planck time series of causal diamonds, i.e. time intervals, on the other.

Let $\delta_{AB}(t)$ and $\delta_{BA}(t)$ denote the time series of discrete projections of these operators onto a common classical emergent time variable t, again associated with the AB, BA directions. They correspond physically to combinations of noncommuting operators that measure in the orthogonal directions, as discussed below. Each series represents a realization of quantum noise with a Planck spectral density, with one bit of information per Planck time. Since the states of the two world lines are entangled, the time series are not independent. As illustrated in Fig. (10) for a causal diamond on an interval defined by two times on A in flat space, realizations of the time series on the two world lines relate to each other with a spooky nonlocal correlation:

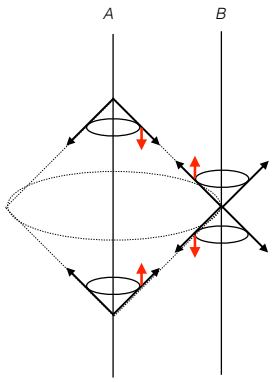

FIG. 10. Causal relationship of entangled light cones for two world lines A and B in flat space-time, adapted from ref.[15]. Eigenvalues for these light cones of the relational antisymmetric phase displacement operators (Eq. 57), $\hat{\delta}^{\pm}_{AB}$ and $\hat{\delta}^{\pm}_{BA}$, are shown schematically by arrows. The causal diamond state in A's frame describes exotically-cancelling virtual past and future displacements, associated with the AB direction, that appear as time-odd displacements in B's frame (Eq. 58). The cross correlation of causal diamond states describes virtual quantum fluctuations in the relationship of proper time between the world lines[13].

$$2\delta_{BA}(t) = \delta_{AB}(t - R/c) - \delta_{AB}(t + R/c), \tag{58}$$

where R is the separation. The same relation applies with A and B reversed.

Eqs. (57) and (58) express the idea that virtual time displacements of A relative to B represent Planck scale fluctuations of "borrowed time" that are "paid back" after a round trip light crossing time, and *vice versa*. It is the counterpart of the antisymmetry of the nonlocal operators $\hat{\delta}_{i\pm}$ and $\delta\hat{\tau}_i$, assigned to causal diamonds for different observers in the same space-time (Eqs. 12 and 17).

This relationship between time series leads to a purely imaginary cross spectrum in the frequency domain,

$$\tilde{\delta}_{BA}(f) \;=\; i\,\sin(2\pi f R/c)\;\tilde{\delta}_{AB}(f). \tag{59}$$

The cross spectrum between the world lines is imaginary because the cross correlation represents pure entanglement information— it is not visible in the autocorrelation of either time series with itself, only when the two are compared. The offset phase between them is always 90 degrees, but the actual phase is determined by the state preparation— in this case, environmental information associated with the states of the spatial directions orthogonal to $\vec{AB}$.

Time antisymmetry in antipodal directions is also found in a consistent quantum model[10–12] of inbound and outbound particle states of an eternal quantum black hole event horizon (Fig. 2). That particular model does not explicitly treat holographic directional correlations, as it only quantizes the radial part of the back-reaction of quantized particle states on the metric. On the other hand, directional quantization must exist in some form to be consistent with black hole entropy. If the hypothesis of this paper about the inflationary horizon is correct, the nonlocal holographic information in quantized states of black hole horizons should produce directional entanglement, correlations and fluctuations similar to those discussed above (e.g., Eq. 16).

A similar relation was used in ref.[15] to model experimental cross spectra of interferometers. In that application, the cross spectrum of two signals is imaginary Planck amplitude noise, filtered on a scale R determined by a set of mirrors used to project directional states of propagating light onto a data stream in the classical proper time of a single laboratory rest frame. If spooky cosmological correlations are detected, it is likely that Planck scale correlations could be measured in suitably configured experiments[39–42].

In our extrapolation to inflation, classical cosmic time is determined by the time component ($\nu = 0$) of the classical timelike vector u^ν_ϕ defined for each world line by the unperturbed inflationary metric, as discussed above (Eq. 36). The antisymmetry in observable 3D spatial perturbations follows from general covariance, by projection into 3D comoving transform space (Eqs. 36 and 37). Our model is that the fluctuations become "frozen in time" when an emergent perturbation crosses the horizon, leaving an image on the frozen classical metric of antisymmetric Planck amplitude noise filtered at $f \approx H$.

The argument just given refers to a classical laboratory time t, but a consistent theory must define relations between concrete observables. It is useful to contrast our quantum-time measurement with Einstein's classical thought experiment in which "light clocks" measure ticks of local proper time by bouncing light between mirrors at fixed separation in a rest frame. That experiment shows how relativistic time dilation occurs: two observers in relative motion who compare clocks both see the other's clock ticking slowly, because light has to travel farther to accommodate apparent position displacements in the moving frame. Here, the output of a light clock corresponds to a directionally oriented time operator, similar to $\hat{\delta}_{i\pm}$ or $\Delta\hat{\tau}_i$; signals of light clocks in different directions do not commute, and comparisons of three directions obey a spin-like algebra like that studied above, where the operator $\hat{T}$ represents classical proper time. The time series $\delta_{AB}(t)$, $\delta_{BA}(t)$ can be operationally defined as differences between clocks aligned orthogonally to the AB spatial separation direction, near A and and B world lines respectively. Thus, the exotic relative time fluctuation is not always a dilation, but can have either positive or negative sign, averages to zero for two observers at rest, and is directionally antisymmetric in both space and time.